

# Magnetic-field-induced stepwise director reorientation and untwisting of a planar cholesteric structure with finite anchoring energy

A. N. Zakhlevnykh\* and V. S. Shavkunov

*Physics of Phase Transitions Department, Perm State University, Bukirev Street 15, Perm 614990, Russia*

(Received 24 May 2016; published 28 October 2016)

Within the continuum approach we study the equilibrium configurations of a cholesteric liquid crystal confined between two parallel plates, when a magnetic field is applied perpendicularly to the plates. We analyze the role of soft anchoring boundary conditions on magnetic-field-induced cholesteric-nematic transitions in a finite thickness cholesteric cell, treated to induce soft planar alignment. We study the stepwise behavior of cholesteric pitch as a function of the anchoring energy, the thickness of a layer, and the field strength. We analyze some kinds of soft anchoring potentials, including the case of degeneration of the easy axes. We show that the variation of the thickness or intrinsic pitch induces the stepwise behavior of a pitch of the planar cholesteric structure, and the stepwise variations of the average tensor of diamagnetic susceptibility. The values of these jumps are determined by the anchoring energy. We find the values of critical parameters for the transitions between planar and confocal cholesteric states, and homeotropic nematic state. We show that the variation of the anchoring energy leads to change of the phase transition character; the conditions for hysteresis behavior are obtained. We show that for rather soft anchoring the confocal state is metastable, and the increase of a magnetic field leads to the direct transition between the planar cholesteric and homeotropic nematic phases. We also give a detailed derivation of the threshold and saturation properties of planar cholesteric to homeotropic nematic transition.

DOI: [10.1103/PhysRevE.94.042708](https://doi.org/10.1103/PhysRevE.94.042708)

## I. INTRODUCTION

Optical properties of liquid crystal (LC) cells are determined by the type of their structure, i.e., spatial distribution of a director field  $\mathbf{n}(\mathbf{r})$  [here  $\mathbf{n}$  is the unit vector along which the main axes of the molecules are oriented on the average]; therefore, the study of possible types of structures and features of orientational transitions under the action of external magnetic or electric fields is an actual problem in the physics of liquid crystals.

It is known that the type of a LC structure depends on material parameters, on the direction and strength of external fields, and also on the orientation of the director on the boundaries of a layer [1,2]. The orientation of the director near the surface is determined by the method of its fabrication and by the material it is made of. Depending on these factors, it is energetically favorable for the director to be oriented along some direction called an easy orientation axis. In the simple case of a flat surface the axis of the easy orientation is directed more often along a normal to a surface (homeotropic orientation) or perpendicular to the surface (planar orientation). If the director alignment on the boundaries of the layer is strictly determined (so-called rigid or strong anchoring), the director on a surface coincides with the axis of the easy orientation. However, for a more exact description of the spatial distribution of the director field in a cell, as shown in Ref. [3], it is necessary to suppose that the anchoring energy is finite (soft anchoring), and consequently external fields can cause deviations of the director  $\mathbf{n}(\mathbf{r})$  from the easy orientation direction. In a nematic LC the conditions for coupling of molecules with the surface provide the orientation of the director in a cell. In the case of cholesteric liquid crystals

(CLCs) the orientation of the director in a cell also depends on the twisting ability of its molecules (or optically active dopant); therefore, the helical director structure is formed with some pitch.

Variation of parameters of the system influencing the spatial distribution of a director field in a cell can cause the spiral cholesteric structure to disappear: there will be a phase transition into the nematic state. For example, in a CLC with diamagnetic anisotropy  $\chi_a > 0$  a relatively high magnetic field, directed along a normal to the boundaries of a layer on which soft planar anchoring for the director takes place, causes the phase transition into a homeotropic nematic state, in which the director in a cell is oriented along the direction of a magnetic field (the so-called saturation state). Depending on the type of CLC alignment, in the absence of a magnetic field this phase transition into the nematic state can occur in several ways.

The problem of the concrete form of interaction energy of LC molecules with a bounding surface is one of the key questions in the physics of liquid crystals. Now there are plenty of works devoted to the study of the influence of this interaction on orientational properties of a LC in a layer [3–30]. The authors of these works, however, more often deal with nematics [3–9] or cholesterics with strong anchoring conditions at the boundaries of a layer [14–19,31].

Nowadays there are a lot of ways of treating the surfaces to allow the creation of some axes of easy orientation on them [4,9]. Thus, there is an opportunity to set various orientations of LC molecules on the boundaries of a layer by changing the values of the system parameters (thickness of a layer, or magnetic or electric field strength).

In the present paper a cholesteric-nematic phase transition in the plane-parallel cell placed in homogeneous magnetic field, directed along a normal to a plane of a cell, is studied. It is supposed that the axes of easy orientation are located

\*anz@psu.ru

in the plane of the layer boundaries and directed under some angle to each other; i.e., in the absence of a magnetic field there is a planar cholesteric structure in the layer with the helical axis along a normal to the boundaries of a cell. Diamagnetic anisotropy  $\chi_a$  of a cholesteric is assumed to be positive; therefore, the growth of magnetic field strength causes distortions of the initial planar cholesteric structure, i.e., the reorientation of a director field in the layer, that results (in a strong enough magnetic field) in a transition into a homeotropic nematic state in which the director in a cell is oriented along a magnetic field direction (the saturation state).

Problems similar to those described above are investigated now rather intensively (see, for instance, Refs. [10–13,20–23]). In these papers expressions were obtained which determine the threshold Fréedericksz field. It was shown that due to a finite anchoring energy the homeotropic nematic state (the saturation state) can exist in the cell, and the saturation field was derived, for which such a nematic state must exist. However, in the majority of works the authors for the description of a planar cholesteric state in a cell assumed the total turn of the director around the helical axis to have a constant value, which does not depend on the thickness of a cell. Such an approach is rather good for studying the orientational properties of nematic plane-parallel twist cells in which the turn of the director in a layer is determined by the relative angle of rotation of the layer boundaries. It is known [1,2] that in a planar cholesteric state the integer number of half turns of a spiral structure can be in a layer. It means that the total angle of the director rotation in the layer can accept a discrete number of allowable values determined by the distance between the boundaries of the layer, the intrinsic pitch of the helical structure, and the anchoring energy at the boundaries of the layer [24,25]. As it is shown below, this allows one to describe the unwinding of a helical cholesteric structure at the cholesteric-homeotropic nematic phase transition under the action of a magnetic field directed along the spiral axis of a cholesteric. In the present paper we analyze several types of anchoring potentials, including the potential with the degeneration of the easy orientation axis.

Let us also note the great interest in the investigation of stepwise variation of the helical pitch induced by different factors: anchoring or temperature-induced stepwise behavior [24–30,32–34] or light-induced stepwise behavior [35–39] of the pitch. The magnetic-field-induced stepwise untwisting of the cholesteric structure was studied in Refs. [40,41] under strong anchoring conditions. Anchoring energy effects on the stability of CLC helical structures in the field absence were investigated in Refs. [42,43].

The paper is organized as follows. In Sec. II, we derive the governing equations describing the planar cholesteric cell with soft anchoring boundaries under the magnetic field action. Unlike Refs. [10–13,20–23] we consider not only the possibility of a transition between the planar and distorted states (the Fréedericksz transition), but also the stepwise behavior of a cholesteric spiral structure in relatively thick layers, as well as the transition into a saturation (nematic) state. In Sec. III, we study the influence of the polar anchoring strength. The influence of the degeneration of the easy orientation axis on the cholesteric-nematic transition is studied in Sec. IV. Finally, Sec. V is devoted to conclusions.

## II. PLANAR ANCHORING

### A. Equations of equilibrium

Consider a CLC layer of thickness  $d$  confined between two parallel plates. Let us direct the  $z$  axis perpendicularly to the layer, so  $z = 0$  corresponds to the bottom boundary and  $z = d$  to the top boundary. We direct the external magnetic field along the normal to the layer  $\mathcal{H} = (0, 0, \mathcal{H})$ , and the diamagnetic anisotropy  $\chi_a$  is assumed to be positive. The components of the director can be written as

$$\mathbf{n} = (\cos \theta \cos \varphi, \cos \theta \sin \varphi, \sin \theta), \quad (1)$$

where the polar angle  $\theta$  is measured from the plane of the layer, and the azimuthal angle  $\varphi$  is measured from the  $x$  axis directed along the layer. We assume the angles  $\theta$  and  $\varphi$  to be the functions of the  $z$  coordinate.

The distribution of the director field in the layer of cholesteric LC is determined from the conditions of the minimum of the free energy functional

$$\mathcal{F} = \int F_v dV + \int F_S dS, \quad (2)$$

where the volume density of the free energy  $F_v$  is given by the expression [1]

$$F_v = \frac{1}{2} [K_{11}(\nabla \mathbf{n})^2 + K_{22}(\mathbf{n} \cdot \nabla \times \mathbf{n} + q_0)^2 + K_{33}(\mathbf{n} \times \nabla \times \mathbf{n})^2] - \frac{1}{2} \chi_a (\mathbf{n} \cdot \mathcal{H})^2, \quad (3)$$

and  $F_S$  is the surface density of the interaction energy of cholesteric molecules with the boundaries, which can be written as [3]

$$z = 0: F_S = -\frac{W_a}{2} (\mathbf{n} \cdot \mathbf{e}_{s1})^2, \quad (4)$$

$$z = d: F_S = -\frac{W_a}{2} (\mathbf{n} \cdot \mathbf{e}_{s2})^2. \quad (5)$$

Here the modules of the orientational elasticity  $K_{11}$ ,  $K_{22}$ , and  $K_{33}$  are positive and characterize splay, twist, and bend deformations, respectively;  $q_0$  is the wave number of the intrinsic helical structure ( $q_0 \equiv 0$  for nematics);  $W_a > 0$  is the surface density of the azimuthal energy of coupling of cholesteric molecules with the boundaries of a cell; and  $\mathbf{e}_{s1}$  and  $\mathbf{e}_{s2}$  are the unit vectors of easy orientation at the bottom and top surfaces, respectively:

$$\mathbf{e}_{s1} = (\cos \beta, -\sin \beta, 0), \quad \mathbf{e}_{s2} = (\cos \beta, \sin \beta, 0). \quad (6)$$

The angle  $\beta$  is measured from the  $x$  axis, so the axes of easy orientation lying in the planes of the top and bottom surfaces are oriented under an angle  $2\beta$  to each other.

Choosing  $q_0^{-1}$  as the unit of length, and  $\mathcal{H}_q = q_0 \sqrt{K_{11}/\chi_a}$  as the unit of magnetic field strength, so the dimensionless magnetic field  $H = \mathcal{H}/\mathcal{H}_q$ , we can substitute the director (1) in Eq. (3) and obtain

$$\begin{aligned} \frac{F_v}{K_{11}q_0^2} = \frac{1}{2} \{ & f(\theta)\dot{\theta}^2 + h(\theta)\dot{\varphi}^2 - 2k_2\dot{\varphi} \cos^2 \theta \\ & - H^2 \sin^2 \theta + k_2 \}, \end{aligned} \quad (7)$$

where

$$\begin{aligned} f(\theta) &= \cos^2 \theta + k_3 \sin^2 \theta, \\ h(\theta) &= (k_2 \cos^2 \theta + k_3 \sin^2 \theta) \cos^2 \theta. \end{aligned}$$

In Eq. (7) the dot designates the differentiation on the dimensionless coordinate  $\tilde{z} = q_0 z$  and the following dimensionless parameters are used:

$$k_2 = \frac{K_{22}}{K_{11}}, \quad k_3 = \frac{K_{33}}{K_{11}}, \quad (8)$$

where the tilde above the dimensionless coordinate is omitted below.

The surface densities of the free energy, Eqs. (4) and (5), can be written as

$$z = 0: \quad \frac{F_S}{K_{11}q_0} = -\frac{w}{2} \cos^2 \theta \cos^2(\beta + \varphi), \quad (9)$$

$$z = D: \quad \frac{F_S}{K_{11}q_0} = -\frac{w}{2} \cos^2 \theta \cos^2(\beta - \varphi). \quad (10)$$

Here  $D = q_0 d$  is the dimensionless thickness of the layer, and  $w = W_a/(K_{11}q_0)$  is the dimensionless anchoring energy. We assume that the functions  $\varphi(z)$  and  $\theta(z)$  have the following properties [13]:

$$\theta(z) = \theta(D - z), \quad \varphi(z) = 2\varphi_m - \varphi(D - z), \quad (11)$$

where  $\varphi_m \equiv \varphi(D/2)$ . It follows from Eq. (11) that

$$\dot{\theta}(z = 0) = -\dot{\theta}(z = D), \quad \dot{\varphi}(z = 0) = \dot{\varphi}(z = D), \quad (12)$$

$$\theta(0) = \theta(D) \equiv \theta_S, \quad \varphi(0) \equiv -\varphi_S = 2\varphi_m - \varphi(D), \quad (13)$$

$$\theta(D/2) \equiv \theta_m, \quad \dot{\theta}(D/2) = 0, \quad (14)$$

and the total variation  $\Delta\varphi$  of the azimuthal angle on the thickness of a layer is equal to

$$\Delta\varphi = \varphi(z = D) - \varphi(z = 0) = 2(\varphi_m + \varphi_S). \quad (15)$$

Minimization of the free energy functional (2) over  $\theta(z)$  and  $\varphi(z)$  results in the following equations:

$$\begin{aligned} \frac{d}{dz}[f(\theta)\dot{\theta}] &= \frac{1}{2} \frac{\partial}{\partial \theta}[f(\theta)\dot{\theta}^2] + \frac{1}{2} \dot{\varphi}^2 \frac{\partial}{\partial \theta} h(\theta) \\ &\quad + k_2 \dot{\varphi} \sin 2\theta - H^2 \sin 2\theta, \end{aligned} \quad (16)$$

$$\dot{\theta} \dot{\varphi} \left[ \frac{\partial}{\partial \theta} h(\theta) \right] + h(\theta) \ddot{\varphi} + k_2 \dot{\theta} \sin 2\theta = 0, \quad (17)$$

and boundary conditions

$$z = 0: \quad -\frac{\partial F_v}{\partial \theta} + \frac{\partial F_S}{\partial \theta} = 0, \quad -\frac{\partial F_v}{\partial \varphi} + \frac{\partial F_S}{\partial \varphi} = 0, \quad (18)$$

$$z = D: \quad \frac{\partial F_v}{\partial \theta} + \frac{\partial F_S}{\partial \theta} = 0, \quad \frac{\partial F_v}{\partial \varphi} + \frac{\partial F_S}{\partial \varphi} = 0. \quad (19)$$

Let us rewrite Eqs. (18) and (19), using Eqs. (7) and (9)–(11):

$$\begin{aligned} z = 0: \quad & -f(\theta_S)\dot{\theta} + \frac{w}{2} \sin 2\theta_S \cos^2(\beta - \varphi_S) = 0, \\ & -h(\theta_S)\dot{\varphi} + k_2 \cos^2 \theta_S + \frac{w}{2} \cos^2 \theta_S \sin 2(\beta - \varphi_S) = 0, \end{aligned} \quad (20)$$

$$\begin{aligned} z = D: \quad & f(\theta_S)\dot{\theta} + \frac{w}{2} \sin 2\theta_S \cos^2(\beta - 2\varphi_m - \varphi_S) = 0, \\ & -h(\theta_S)\dot{\varphi} + k_2 \cos^2 \theta_S + \frac{w}{2} \cos^2 \theta_S \\ & \times \sin 2(\beta - 2\varphi_m - \varphi_S) = 0. \end{aligned} \quad (21)$$

As it is seen, Eqs. (20) and (21) coincide provided that the angle  $\varphi_m$  accepts a discrete series of values

$$\varphi_m = n\pi/2, \quad (22)$$

where  $n$  is an integer, having, as shown below, the sense of the number of half turns of a cholesteric spiral structure, which can be determined from the condition of the minimum of the total energy, Eq. (2).

In Refs. [13,20,24,25,38,44–46] the phase transition between the planar cholesteric and the homeotropic nematic phases in a layer with planar anchoring of the director at the boundaries, in electric or magnetic fields oriented perpendicularly to the boundaries of the layer, was considered. The parameter  $\varphi_m$  in these works can have appropriate values: in Refs. [13,20] (in which  $\beta = 0$ ) the angle  $\varphi_T = 2\varphi_m$  takes the values  $3\pi/2$  and  $\pi/2$ ; in Ref. [46] the parameter  $\varphi_{\text{eff}} = 2\varphi_m$  takes the values from the interval  $(50^\circ, 130^\circ)$ . However, according to Eq. (22), the angles  $\varphi_T$  and  $\varphi_{\text{eff}}$  can have only the discrete values  $n\pi$ , where  $n$  can accept only integer values determined by the minimum of the total energy, Eq. (2).

As it is easy to see, for all values of material parameters of the system, the thickness of a layer, and the magnetic field strength, Eqs. (16), (17), (20), and (21) have two trivial solutions

$$\theta(z) \equiv 0 \quad \text{and} \quad \theta(z) \equiv \pi/2. \quad (23)$$

The former corresponds to the planar cholesteric state, and the latter corresponds to the homeotropic nematic state. At  $\theta(z) \equiv 0$  from Eqs. (16) and (11) it follows that

$$\varphi(z) = qz - \varphi_S, \quad \text{where} \quad q = 2(\varphi_m + \varphi_S)/D, \quad (24)$$

and the value  $\varphi_S$  at a given thickness of the layer  $D$  is determined from Eq. (20):

$$D = \frac{4k_2(\varphi_m + \varphi_S)}{2k_2 + w \sin 2(\beta - \varphi_S)}. \quad (25)$$

The expression for the dimensionless total energy (2) in the planar state  $\mathcal{F}_0 \equiv \mathcal{F}/(K_{11}q_0S)$  becomes

$$\mathcal{F}_0 = \frac{D}{8k_2} w^2 \sin^2 2(\beta - \varphi_S) - w \cos^2(\beta - \varphi_S). \quad (26)$$

Here  $S$  is the surface area of the layer boundaries.

In the case of homeotropic nematic ordering [ $\theta(z) \equiv \pi/2$ ] the director  $\mathbf{n}$  is oriented along the direction of a magnetic field, and the total energy (2) is equal to

$$\mathcal{F}_{\pi/2} \equiv \frac{\mathcal{F}}{K_{11}q_0S} = \frac{1}{2} D(k_2 - H^2). \quad (27)$$

Together with the trivial solutions (23), Eqs. (16) and (20) have nontrivial solution  $0 < \theta(z) < \pi/2$ , corresponding to a confocal cholesteric phase for which the director makes the angle  $\theta(z)$  with the spiral axis. Now we write the expressions describing the distribution of a director field in this phase.

As seen from Eqs. (7), (9), and (10), the total energy (2) does not depend explicitly on  $z$  and  $\varphi$ . This allows us to write the first integrals

$$C_1 = \dot{\theta} \frac{\partial F_v}{\partial \dot{\theta}} + \dot{\varphi} \frac{\partial F_v}{\partial \dot{\varphi}} - F_v = f(\theta) \dot{\theta}^2 + h(\theta) \dot{\varphi}^2 + H^2 \sin^2 \theta, \quad (28)$$

$$C_2 = \frac{\partial F_v}{\partial \varphi} = h(\theta) \dot{\varphi} - k_2 \cos^2 \theta, \quad (29)$$

where  $C_1$  and  $C_2$  are constants of integration [Eqs. (28) and (29) can be received directly from Eqs. (16), and (17)]. Expressing  $\dot{\varphi}$  from Eq. (29) and substituting it in Eq. (28), we find the value of the constant  $C_1$  with the help of Eq. (14):

$$C_1 = \frac{(C_2 + k_2 \cos^2 \theta_m)^2}{h(\theta_m)} + H^2 \sin^2 \theta_m, \quad (30)$$

where  $\theta_m \equiv \theta(D/2)$ .

Equation (20) for the angle  $\varphi$  determines the value of constant  $C_2$ :

$$C_2 = \frac{w}{2} \cos^2 \theta_S \sin 2(\beta - \varphi_S). \quad (31)$$

Expressing the derivatives  $\dot{\theta}$  and  $\dot{\varphi}$  from Eqs. (28) and (29) and using Eqs. (30) and (31) we can write the equations for  $\theta(z)$  and  $\varphi(z)$ :

$$z = \int_{\theta_S}^{\theta(z)} \sqrt{A(\theta)} d\theta, \quad (32)$$

$$\varphi(z) + \varphi_S = \int_{\theta_S}^{\theta(z)} \frac{(C_2 + k_2 \cos^2 \theta)}{h(\theta)} \sqrt{A(\theta)} d\theta, \quad (33)$$

where

$$A(\theta) = f(\theta) \left/ \left\{ \frac{(C_2 + k_2 \cos^2 \theta_m)^2}{h(\theta_m)} - \frac{(C_2 + k_2 \cos^2 \theta)^2}{h(\theta)} + H^2 (\sin^2 \theta - \sin^2 \theta_m) \right\} \right. \quad (34)$$

The values of the quantities  $\theta_m$  and  $\varphi_S$  are determined from the expressions

$$\frac{D}{2} = \int_{\theta_S}^{\theta_m} \sqrt{A(\theta)} d\theta, \quad (35)$$

$$\varphi_m + \varphi_S = \int_{\theta_S}^{\theta_m} \frac{(C_2 + k_2 \cos^2 \theta)}{h(\theta)} \sqrt{A(\theta)} d\theta, \quad (36)$$

following from Eqs. (32) and (33). The first equation in Eq. (20) together with Eqs. (28), (30), and (31) determines the value of  $\theta_S$ :

$$\frac{f(\theta_S)}{\sqrt{A(\theta_S)}} = \frac{w}{2} \sin 2\theta_S \cos^2(\beta - \varphi_S). \quad (37)$$

Thus, Eqs. (32)–(37) and (22) describe the distribution of the CLC director in a confocal phase. The integer number  $n$  in Eq. (22) is determined from the condition of the minimum of the total energy (2), the expression for which becomes as

follows:

$$\mathcal{F}_\theta = \int_{\theta_S}^{\theta_m} \left\{ \frac{f(\theta)}{\sqrt{A(\theta)}} + \left[ \frac{(C_2^2 - k_2^2 \cos^4 \theta)}{h(\theta)} - H^2 \sin^2 \theta \right] \sqrt{A(\theta)} \right\} d\theta + \frac{1}{2} k_2 D - w \cos^2 \theta \cos^2(\beta - \varphi_S). \quad (38)$$

### B. Planar state

As seen from Eq. (24), in the planar state the pitch of the spiral  $p = 2\pi/q$ , generally speaking, is not equal to the intrinsic pitch  $p_0 = 2\pi$  of a cholesteric (in the dimensional form  $p_0 = 2\pi/q_0$ ), and for the given thickness of a layer it should satisfy the relation

$$D = \frac{p}{2} n + \frac{p}{\pi} \varphi_S, \quad (39)$$

which follows from Eqs. (22) and (24). In accordance with Eq. (39), the integer number  $n$  of half turns of a spiral [see the first item in Eq. (39)] should be placed in the layer of thickness  $D$ . The second item in Eq. (39) corresponds to that part of the spiral structure where the director rotates at an angle  $2\varphi_S$  (the angle between the orientations of the director at the bottom and top surfaces).

In a particular case, when the pitch of the spiral of the planar structure coincides with the intrinsic pitch  $p_0$ , as it follows from Eqs. (22) and (24),  $\dot{\varphi} = 1$  (or in dimensional units  $\dot{\varphi} = q_0$ ), and the thickness of the layer satisfies the relation

$$D = \pi t + 2\beta, \quad (40)$$

where  $t$  is some integer. In this case  $\varphi_S = \beta$ ; i.e., there is no deviation of the director orientation from the easy axes on the top and bottom boundaries, the variation of the azimuthal angle (15)  $\Delta\varphi = 2(\varphi_m + \beta) = \pi t + 2\beta$ , and the total energy (26) reaches the minimal value  $\mathcal{F}_0 = -w$ .

In the case when Eq. (40) is not satisfied, i.e.,  $t$  is some fractional number, the spectrum of allowable values of  $\varphi_m$  will be determined by expression (22), in which  $n$  is an integer [see Eq. (39)], which is determined by the minimum of expression (26). In accordance with the aforesaid, between the values of angles  $\varphi_S$  and  $\beta$  and the numbers  $n$  and  $t$  the following relation holds:

$$(\beta - \varphi_S) \sim (n - t), \quad (41)$$

where  $n$  is a positive integer, and  $t$  is any positive number determined by expression (40). Hence, the total energy (26)

$$\mathcal{F}_0 \sim (n - t)^2 \quad (42)$$

will have a minimum at  $n = t$  if  $t$  is an integer (the pitch of the spiral is equal to the equilibrium pitch  $p_0$ ), otherwise it will have a minimum at  $n$  equal to  $t$  approximated up to the nearest integer. Thus, in the planar state the value of an integer  $n$  in Eq. (22) is determined by the expression

$$n = \left\| \frac{(D - 2\beta)}{\pi} \right\|, \quad (43)$$

which together with Eqs. (25) and (26) determines the minimum of the CLC total energy in the planar state (here

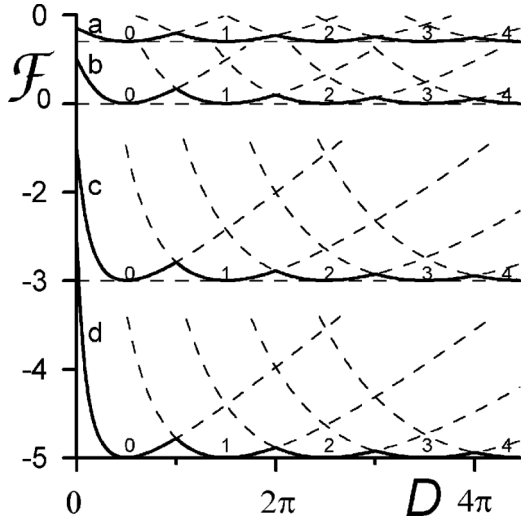


FIG. 1. Dependence of  $\mathcal{F}_0$  on the thickness of the layer  $D$  for  $k_2 = 0.6$ ,  $k_3 = 1.5$ , and  $\beta = \pi/4$ : (a)  $w = 0.3$ , (b)  $w = 1$ , (c)  $w = 3$ , and (d)  $w = 5$ .

$\|\dots\|$  is the designation for the rounding off up to the nearest integer). We notice that if the thickness  $D \rightarrow 0$ , i.e., for dimensional values the condition  $d/p_0 \ll 1$  is satisfied, the total rotation of the director (15) will be determined only by the relative turn of the layer boundaries, i.e., by the angle  $\Delta\varphi = 2\beta$  in the case  $w = \infty$  or  $\Delta\varphi = 2\varphi_S$  in the case  $w \neq \infty$ . For a nematic  $d/p_0 = 0$ ; therefore, the angle  $\varphi_m \equiv 0$ . The authors of Ref. [13], however, consider the special cases of a planar structure in a nematic and set an incorrect value  $\varphi_t = \pi/2$  for the angle  $\varphi_t = 2\varphi_m$ .

In Fig. 1 the total free energy of a cholesteric in the planar state  $\mathcal{F}_0$  is shown as a function of the thickness of a layer  $D$  for  $\beta = \pi/4$  at various values of anchoring energy  $w$  (in the computations we use the set of material parameters [13,20]  $k_2 = 0.6$ ,  $k_3 = 1.5$ ). For each value of  $w$  the family of curves [see Figs. 1(a)–1(d)] is shown, which consists of dashed lines and one thick line. Each dashed line is the solution of Eqs. (25) and (26) for which the angle  $\varphi_m$  takes one of the allowable values determined by Eq. (22) (the integer indices in Fig. 1 correspond to the values of  $n$ ). As seen from Fig. 1, each dashed line corresponding to one of the allowable values of  $\varphi_m$  has one minimum, which is achieved when Eq. (40) is satisfied, and at further increase of the thickness  $D$  the free energy infinitely increases. Dashed lines in each family intersect; therefore, at the increase of the thickness  $D$ , the minimal values of  $\mathcal{F}_0$  correspond to the consecutive transitions from the planar state with  $\varphi_m = 0$  (dashed curve 0) to the state with  $\varphi_m = \pi/2$  (dashed curve 1), which then is replaced with the state with  $\varphi_m = \pi$  (dashed curve 2), etc. Just the same process of change of  $\varphi_m$  with the growth of the thickness  $D$ , corresponding to the minimum of the total energy  $\mathcal{F}_0$ , is determined by Eqs. (22), (25), (26), and (43) (see also the thick lines in Fig. 1). As seen from Fig. 1, for any value of  $w$  the transition from the planar cholesteric state with  $\varphi_m = n\pi/2$  to the state with  $\varphi_m = (n+1)\pi/2$ , in accordance with Eq. (43), occurs at  $D = 2\beta + \pi(n+1/2)$ , i.e., at the increase of the layer thickness by  $\Delta D = \pi$  (or in dimensional units  $\Delta d = p_0/2$ , where  $p_0$  is the intrinsic pitch of a cholesteric spiral).

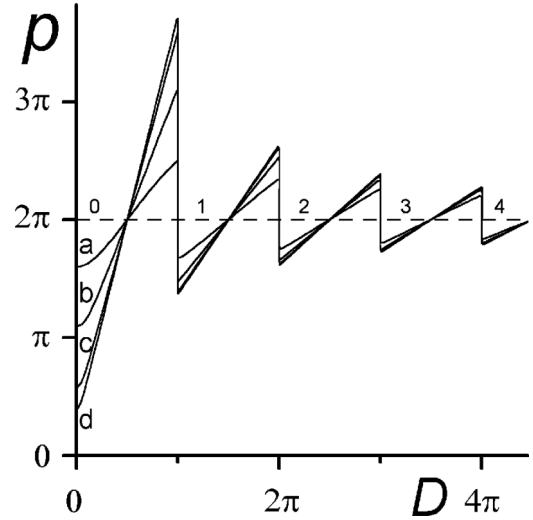


FIG. 2. Dependence of the pitch of spiral  $p$  on the thickness of the layer  $D$  in the planar state for  $k_2 = 0.6$ ,  $k_3 = 1.5$ , and  $\beta = \pi/4$ : (a)  $w = 0.3$ , (b)  $w = 1$ , (c)  $w = 3$ , and (d)  $w = 5$ .

In Figs. 2 and 3 the spiral pitch  $p$  and the angle  $\varphi_S$  are shown as functions of the layer thickness  $D$  in the planar state for different values of anchoring energy  $w$ . The dependencies  $\varphi_S(D)$  and  $p(D)$  are the solutions of the set of equations (22), (25), (39), and (43) and correspond to the minimum of the total energy  $\mathcal{F}_0$  [the integer indices in Figs. 2 and 3 correspond to the values that take  $n$  in Eq. (43) with the increase of the thickness  $D$ ]. As seen from Figs. 2 and 3, at  $D \rightarrow \infty$  the angle  $\varphi_S \rightarrow \beta$ , and the pitch of the spiral tends to the equilibrium value  $p \rightarrow 2\pi$  for an infinite cholesteric (or in dimensional units to the value  $p_0 = 2\pi/q_0$ ). At  $D \rightarrow 0$  the angle  $\varphi_m = 0$  and  $\varphi_S \rightarrow 0$  (see Fig. 3); thus, the pitch of the spiral has the finite value

$$p = 2\pi \frac{D}{\Delta\varphi} \rightarrow 2\pi \frac{D}{2\varphi_S} = \frac{4k_2\pi}{(2k_2 + w \sin 2\beta)}. \quad (44)$$

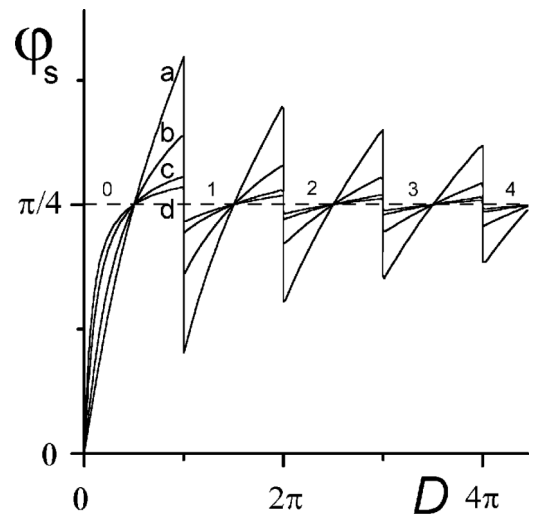


FIG. 3. Dependence of  $\varphi_S$  on the layer thickness  $D$  in the planar state for  $k_2 = 0.6$ ,  $k_3 = 1.5$ , and  $\beta = \pi/4$ : (a)  $w = 0.3$ , (b)  $w = 1$ , (c)  $w = 3$ , and (d)  $w = 5$ .

From Figs. 2 and 3 it is seen that the less the anchoring energy, the more slowly the angle  $\varphi_S \rightarrow \beta$ , but the faster  $p \rightarrow 2\pi$ .

The stepwise behavior of the angle  $\varphi_S$  and the pitch of the spiral  $p$  at the transition between the states distinguished on one half turn of the spiral at  $D = 2\beta + \pi(n + 1/2)$  results in jumps of the average over the layer transverse components of the magnetic susceptibility tensor  $\langle \chi_{ij} \rangle$ :

$$\begin{aligned} \langle \chi_{ij} \rangle &= \frac{1}{D} \int_0^D (\chi_{\perp} \delta_{ij} + \chi_a n_i n_j) dz, \\ \Delta \langle \chi_{xx} \rangle &= \langle \chi_{xx}(n) \rangle - \langle \chi_{xx}(n+1) \rangle, \\ \Delta \langle \chi_{yy} \rangle &= \langle \chi_{yy}(n) \rangle - \langle \chi_{yy}(n+1) \rangle, \\ \Delta \langle \chi_{xx} \rangle &= -\Delta \langle \chi_{yy} \rangle \\ &= \frac{\sin 2\varphi_{S_n}}{2(\pi n + \varphi_{S_n})} - \frac{\sin 2\varphi_{S_{(n+1)}}}{2(\pi[n+1] + \varphi_{S_{(n+1)}})}. \end{aligned} \quad (45)$$

The angles  $\varphi_{S_n}$  and  $\varphi_{S_{(n+1)}}$  in Eq. (45) are determined by relation (25):

$$\begin{aligned} D = 2\beta + \pi \left( n + \frac{1}{2} \right) &= \frac{4k_2 \left( \frac{\pi}{2} n + \varphi_{S_n} \right)}{2k_2 + w \sin 2(\beta - \varphi_{S_n})} \\ &= \frac{4k_2 \left( \frac{\pi}{2} [n+1] + \varphi_{S_{(n+1)}} \right)}{2k_2 + w \sin 2(\beta - \varphi_{S_{(n+1)}})}. \end{aligned} \quad (46)$$

It is easy to show from Eq. (46) that the values of the angles  $\varphi_{S_n}$  and  $\varphi_{S_{(n+1)}}$  satisfy the relation

$$\varphi_{S_n} = \beta + \Delta\varphi_n, \quad \varphi_{S_{(n+1)}} = \beta - \Delta\varphi_n, \quad (47)$$

where the positive parameter  $\Delta\varphi_n$  can be found from the equation

$$w = \frac{k_2(\pi - 4\Delta\varphi_n)}{[2\beta + \pi(n + 1/2)] \sin 2\Delta\varphi_n}. \quad (48)$$

As a result, Eqs. (45) and (46) with the help of Eq. (48) can be written as

$$\begin{aligned} \Delta \langle \chi_{xx} \rangle &= -\Delta \langle \chi_{yy} \rangle \\ &= \frac{\sin 2(\beta + \Delta\varphi_n)}{2(\pi n + \beta + \Delta\varphi_n)} - \frac{\sin 2(\beta - \Delta\varphi_n)}{2(\pi[n+1] + \beta - \Delta\varphi_n)}. \end{aligned} \quad (49)$$

Equations (48) and (49) allow us to obtain the relationship between the jumps of transverse components of the tensor  $\langle \chi_{ij} \rangle$  and the azimuthal anchoring energy  $w = W_a/(q_0 K_{11})$ . Thus, by experimental measuring of  $\Delta \langle \chi_{xx} \rangle$  and  $\Delta \langle \chi_{yy} \rangle$  with the help of Eq. (49) one can determine the parameter  $\Delta\varphi_n$  and, substituting it in Eq. (48), estimate  $W_a$ .

Let us note that light-induced stepwise change of the cholesteric helical pitch was studied experimentally and theoretically in Refs. [35–39] as well as the discontinuous change of averaged values of the components of the CLC dielectric susceptibility tensor.

As supposed above, the considered transition between the planar states differing on one half turn of the spiral is not accompanied by slippage of the director on the boundaries of the layer through the anchoring barrier, i.e., without occurrence of a defect (the so-called  $\chi$  lines [25]). For this it is necessary that the energy of coupling must satisfy the inequality [25]  $W_a < 2\pi K_{22}/d$ .

Let us notice that at  $\beta = \pi/4$  and if relation (40) holds, in which  $t = 1$  ( $\varphi_m = \pi/2$ ), the so-called supertwist state can occur in a cell. In this case the easy axes at the bottom and top walls of a layer are oriented under the angle  $\pi/2$  to each other, the pitch of the spiral is equal to the equilibrium value for an undistorted CLC  $p = p_0$ , and the total angle of the director rotation in the layer  $\Delta\varphi = 3\pi/2$ . The layer thickness in supertwist state is  $D = 3\pi/2$  (or in dimensional units  $d/p_0 = 0.75$  [2]). At  $D < 3\pi/2$  or  $D > 3\pi/2$ , as seen from Fig. 3, the angle  $\varphi_S \neq \beta$ ; therefore, the total angle of the director rotation  $\Delta\varphi = 2(\varphi_m + \varphi_S) \neq 3\pi/2$ , and the supertwist state does not occur.

Reference [13] asserts that due to the soft anchoring the supertwist state can be observed not at  $d/p_0 = 0.75$  as described above, but at  $d/p_0 = 0.7$ ; moreover, for the determination of the threshold characteristics in the supertwist state the angle  $\varphi_t = 2\varphi_m$  is assumed to be  $3\pi/2$ , whereas the allowable values  $\varphi_t = \pi n$ , where  $n$  is an integer.

### C. Fréedericksz field

For the calculation of threshold characteristics of the system, at which there is a deformation of a planar cholesteric structure in a layer under the action of the external magnetic field  $H$ , we consider Eqs. (35) and (37) in the limit  $\theta_m \rightarrow 0$  and obtain

$$D = \frac{4k_2(\varphi_m + \varphi_S)}{w \sin 2(\beta - \varphi_S) + 2k_2}, \quad (50)$$

$$\frac{\sqrt{\gamma(\varphi_S)}}{2wk_2 \cos^2(\beta - \varphi_S)} = \cot \left\{ \frac{\sqrt{\gamma(\varphi_S)}(\varphi_m + \varphi_S)}{w \sin 2(\beta - \varphi_S) + 2k_2} \right\}, \quad (51)$$

where

$$\begin{aligned} \gamma(\varphi_S) &= [w \sin 2(\beta - \varphi_S) + 2k_2] \\ &\quad \times [w(2k_2 - k_3) \sin 2(\beta - \varphi_S) - 2k_2 k_3] + 4k_2^2 H_F^2. \end{aligned} \quad (52)$$

As is easily seen, expression (38) for the total energy coincides with Eq. (26) in the limit  $\theta_m \rightarrow 0$ , and expression (50) coincides with Eq. (25); therefore, the angle  $\varphi_m$  in Eqs. (50) and (51), as mentioned in Sec. II B, should be determined from Eqs. (22) and (43). In this case Eqs. (22), (43), (50), and (51) at the given thickness  $D$  and the CLC material parameters determine the so-called Fréedericksz field  $H_F$ , such that at  $H < H_F$  the planar cholesteric state exists, and at  $H \geq H_F$  the transition to the confocal state occurs.

In Figs. 4 and 5 the dependence of  $H_F$  on the thickness  $D$  (see dashed and thick lines with the integer indices) is shown. Each dashed curve represents the solution of Eqs. (50) and (51), for which the angle  $\varphi_m$  accepts one of the allowable values (22) [the integer index in the dashed curve corresponds to the value, which  $n$  has in Eq. (22)]. As noted above, the dependence  $H_F(D)$  is determined by Eqs. (22), (43), (50), and (51); thick lines in Figs. 4 and 5 correspond to this case. As seen from Figs. 4 and 5, the dependence  $H_F(D)$  represents a “step” function, for which the jumps of  $H_F$  occur at  $D = (n + 1)\pi$  (where  $n = 0, 1, 2, \dots$  are the indices in the curves in Figs. 4 and 5).

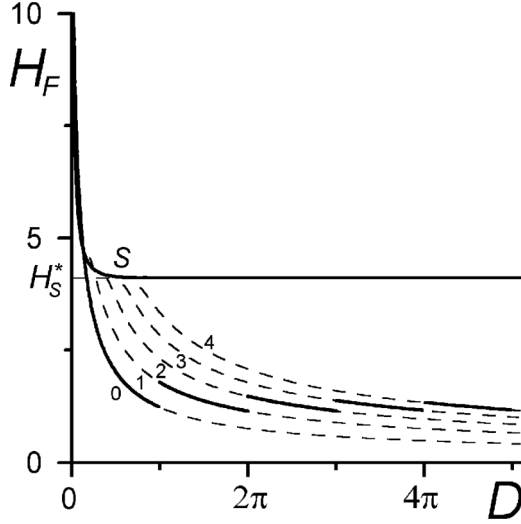


FIG. 4. Dependence of  $H_F$  and  $H_S$  (the curve with the index “S”) on the thickness of the layer  $D$  for  $w = 5$ ,  $k_2 = 0.6$ ,  $k_3 = 1.5$ , and  $\beta = \pi/4$ .

The curves with the index “S” in Figs. 4 and 5 correspond to the saturation field  $H_S$ , such that at  $H > H_S$  there is only a homeotropic nematic state in a layer (the expression for  $H_S$  is reviewed in Sec. IID). In Figs. 4 and 5 two possible situations are shown, when for given thickness  $D$  the saturation field  $H_S > H_F$  (Fig. 4) or  $H_S < H_F$  (Fig. 5). In the first case, as shown below, at a given  $D$  and  $H_F < H < H_S$  the phase transition from the planar cholesteric state to the homeotropic nematic state occurs through the intermediate confocal cholesteric state [ $0 < \theta(z) < \pi/2$ ] and is the second order phase transition. In the second case the given phase transition is always the transition of the first order; i.e., the planar structure at some  $H = H_t^*$  undergoes a stepwise transition in the homeotropic nematic state (the expression for  $H_t^*$  is reviewed in Sec. IIE).

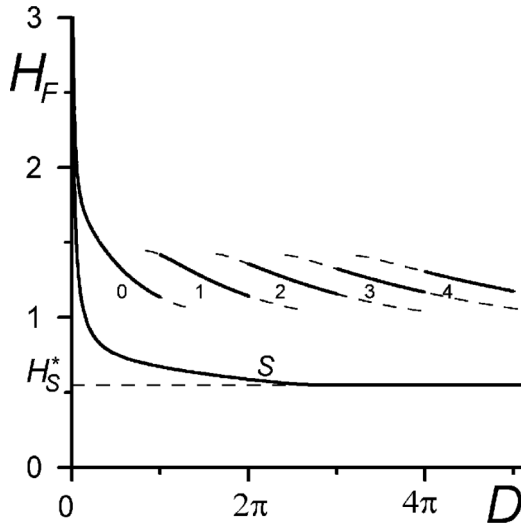


FIG. 5. Dependence of  $H_F$  and  $H_S$  (the curve with the index “S”) on the thickness of the layer  $D$  for  $w = 0.3$ ,  $k_2 = 0.6$ ,  $k_3 = 1.5$ , and  $\beta = \pi/4$ .

As seen from Figs. 4 and 5 (thick lines), at  $D \rightarrow \infty$  the Fréedericksz field  $H_F \rightarrow H_F^*$ . The value of  $H_F^*$  is determined from Eqs. (50) and (51). At  $D \rightarrow \infty$ , as it follows from Eq. (43),  $\varphi_m \rightarrow \infty$ , and  $\varphi_S \rightarrow \beta$  (see Fig. 3); therefore,  $\gamma(\varphi_S) = 4k_2^2(H^2 - k_3)$  [see Eq. (52)], and Eqs. (50) and (51) can be written as

$$\frac{\sqrt{H_F^2 - k_3}}{w} = \cot \left\{ \frac{D}{2} \sqrt{H_F^2 - k_3} \right\}. \quad (53)$$

For  $D \rightarrow \infty$  we obtain

$$H_F^* = \sqrt{k_3}. \quad (54)$$

Let us consider some special cases following from Eqs. (52) and (51). Resolving Eqs. (52) and (51) concerning the magnetic field  $H$ , we obtain within the limits of the rigid planar coupling  $w \rightarrow \infty$  ( $\varphi_{S0} \rightarrow \beta$ ) the threshold value  $H_F$ , known from Ref. [45]:

$$H_F = \frac{1}{D} \{ \pi^2 + 2\beta[2\beta(k_3 - 2k_2) + 2k_2D] \}^{1/2}. \quad (55)$$

The authors of Ref. [45] considered the case  $d/p_0 \ll 1$ ; therefore, the angle  $\varphi_m = 0$  and the total angle of rotation  $\Delta\varphi = 2\beta$ . Within the limits of the rigid coupling ( $w \rightarrow \infty$ ) and  $\beta = 0$  the expression for the threshold value of magnetic field  $H_F$ , determined by Eqs. (52) and (51), takes the form received in Ref. [20]:

$$H_F = \frac{1}{D} \{ \pi^2 + 2\varphi_m[2\varphi_m(k_3 - 2k_2) + 2k_2D] \}^{1/2}. \quad (56)$$

For the case of a twisted nematic cell ( $q_0 = 0$ ) where the total angle of the director rotation on the thickness of a layer is determined only by the relative angle of rotation of bounding plates, i.e.,  $\varphi_m \equiv 0$  and  $\Delta\varphi \equiv 2\beta$ , we obtain the formula known from Ref. [13]:

$$\mathcal{H}_F = \frac{1}{d\sqrt{\chi_a}} \{ K_{11}\pi^2 + 4\beta^2(K_{33} - 2K_{22}) \}^{1/2}. \quad (57)$$

Equation (57) is written in the dimensional form. In the absence of twist in the nematic cell ( $\beta = 0$ ), we obtain the classical Fréedericksz field [1]:

$$\mathcal{H}_F = \frac{\pi}{d} \sqrt{\frac{K_{11}}{\chi_a}}. \quad (58)$$

#### D. Saturation state

Because  $\chi_a > 0$ , at the increase of the magnetic field strength  $H$  the homeotropic nematic state in which the director is oriented along the direction of the magnetic field [ $\theta(z) \equiv \pi/2$ ] should be established in the layer. Reverse decrease of the field, beginning with some value  $H = H_S$ , will cause the deformation of homogeneous homeotropic alignment and a further phase transition from the nematic phase into the cholesteric confocal state. The value  $H_S$  of the field is called the saturation field [13]. For the determination of  $H_S$ , we consider Eqs. (35) and (37) in the limit  $\theta_m \rightarrow \pi/2$ . As a result we obtain the following system of equations for the saturation

state:

$$D = \frac{2k_3}{\sqrt{a}} \ln \left\{ \frac{2\alpha_{S1}\sqrt{a} + \sqrt{4a(\alpha_{S1}^2 + 1) + b^2(\alpha_{S1}^2 + 1)^2}}{\sqrt{4a + b^2(\alpha_{S1}^2 + 1)^2}} \right\}, \quad (59a)$$

$$\varphi_m + \varphi_{S0} = \arctan \left\{ \frac{b\alpha_{S1}^2}{2w \cos^2(\beta - \varphi_{S0})} \right\} + \frac{Dk_2}{2k_3}, \quad (59b)$$

$$\alpha_{S1}\sqrt{4a + b^2(\alpha_{S1}^2 + 1)} = 2w\sqrt{\alpha_{S1}^2 + 1} \cos^2(\beta - \varphi_{S0}), \quad (59c)$$

where  $a = H_S^2 k_3 - k_2^2$  and  $b = w \sin 2(\beta - \varphi_{S0})$ . At the fixed thickness  $D$  and the given values of material parameters, Eqs. (59) determine the value of  $H_S$ , such that at  $H \geq H_S$  there is only the homeotropic nematic phase, and at  $H < H_S$  the phase transition in the confocal cholesteric state takes place. As it is shown below, at  $H \rightarrow H_S$  the value of the angle  $\varphi_m \rightarrow 0$  at any thickness  $D$ ; i.e., the increase of  $H$  causes the unwinding of a spiral structure. In Figs. 4 and 5 the dependencies  $H_S$  on the thickness  $D$  (see curves with the index ‘‘S’’) are shown. As seen from these figures,  $H_S \rightarrow \infty$  at  $D \rightarrow 0$ ; i.e., the reorientation of the director from the planar into the homeotropic state demands infinite  $H_S$ . At  $D \rightarrow \infty$  the magnetic field strength  $H_S \rightarrow H_S^*$  (see Figs. 4 and 5), where  $H_S^*$  is determined by the expression

$$H_S^* = \sqrt{\frac{k_2^2 + w^2}{k_3}}, \quad (60)$$

which follows from Eqs. (59); here  $\varphi_{S0} \rightarrow \beta$  and  $\alpha_{S1} \rightarrow \infty$ .

Equations (59) at  $\beta = 0$  coincide with the system of equations determining the saturation field  $H_S$ , obtained in Ref. [13]. In order to rewrite Eqs. (59) in the form of Ref. [13], it is necessary to introduce the angle  $\beta^0$  according to the relation  $\cos \beta^0 = (\alpha_{S1}^2 + 1)^{-1/2}$ .

### E. Unwinding of a spiral in confocal state

Equations (35)–(33) and (22) determine the distribution of a director field in the confocal cholesteric state, which, as distinct from homeotropic or planar states, can exist only for some interval of values of CLC material parameters, the thickness of a layer, and magnetic field strength. As mentioned in Sec. II A, the integer  $n$  in Eq. (22) should be determined from a condition of a minimum of the total energy (2). In the planar cholesteric state the value of  $n$ , corresponding to a minimum of Eq. (26), is determined by Eq. (43); therefore, for the given thickness  $D$  in the planar state the integer  $n$  is unequivocally determined. However, in the confocal state for given  $n$  it is impossible to obtain the analytical expression similar to Eq. (43); therefore, in order to obtain a real distribution of a director field in the confocal state, it is necessary to find the solutions of Eqs. (32)–(37) and (22) for all possible integers  $n$ , and from the comparison of the total energies (38) of these states to determine the distribution of a director field, possessing the minimal value of  $\mathcal{F}_\theta$ .

In Figs. 6–9 we show  $\theta_m$  as a function of  $H$  at fixed values of CLC material parameters and the thickness of a layer  $D$ , as well as the dependence of the total energies  $\mathcal{F}_\theta$  on  $H$ , which

corresponds to the curves in Figs. 6 and 8. The functions  $\theta_m(H)$  and  $\mathcal{F}_\theta(H)$  are the solutions of Eqs. (35)–(38) and (22). The indices in Figs. 6–9 correspond to the integer values of  $n$  in Eq. (22), the continuous horizontal lines in Figs. 7 and 9 correspond to the value  $\mathcal{F}_0$  [see Eq. (26)], and the dashed line with the index  $\mathcal{F}_{\pi/2}$  corresponds to the total energy in the homeotropic state [see Eq. (27)]. The arrows in Figs. 6 and 8 show the change of the angle  $\theta_m$  at the increase and at the decrease of  $H$ . In Figs. 6 and 7 the thickness  $D = 8$ ; hence, at  $0 \leq H < H_F$  the planar cholesteric state exists in a layer, in which  $\varphi_m = \pi$ , i.e.,  $n = 2$  (see thick curve with index 2 in Fig. 4). The value  $H_F$  is determined by Eqs. (50) and (51). The further increase of  $H$  at  $H \geq H_F$  causes the jumplike change of  $\theta_m$  and  $\varphi_m$ : there is a transition in the confocal state with  $n = 1$ ; i.e., the angle  $\varphi_m$  achieves the value  $\pi/2$  and the half-turn number of a spiral structure decreases by a unit. In this case, as seen from Fig. 7, the energies of the states with  $n = 1$  and  $n = 0$  are close, but the total energy  $\mathcal{F}_\theta$  of the state with  $n = 1$  remains less than the energy  $\mathcal{F}_\theta$  of the state with  $n = 0$ . With the increase of  $H$  at some value  $H_F < H < H_S$  [where  $H_S$  is determined from Eq. (59)] the state with  $n = 1$  transforms into the state with  $n = 0$ : the spiral structure becomes completely untwisted, the angle  $\varphi_m = 0$  and the director in the middle of the layer is oriented along the

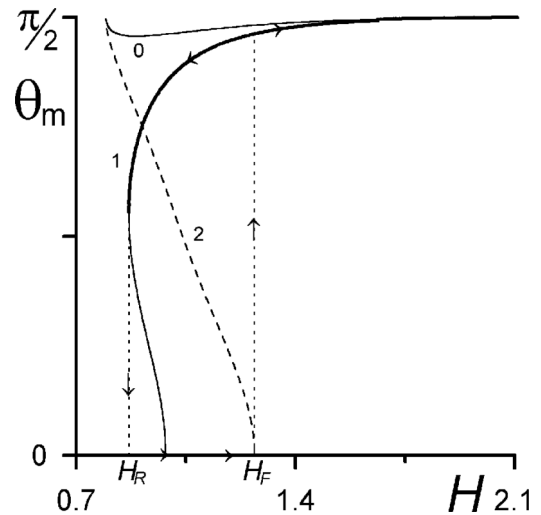


FIG. 6. Dependence of the angle  $\theta_m$  on the magnetic field strength  $H$  for  $w = 5$ ,  $D = 8$ ,  $k_2 = 0.6$ ,  $k_3 = 1.5$ , and  $\beta = \pi/4$ : curve 0,  $n = 0$ , angle  $\varphi_m = 0$ ; curve 1,  $n = 1$ , angle  $\varphi_m = \pi/2$ ; curve 2,  $n = 2$ , angle  $\varphi_m = \pi$ .

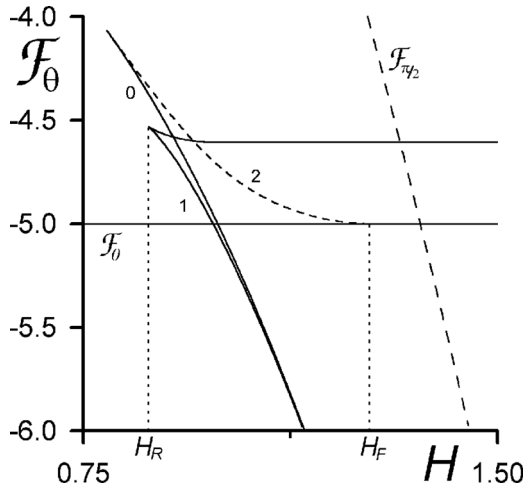


FIG. 7. Dependence of  $\mathcal{F}_\theta$  on the magnetic field strength  $H$  for  $w = 5$ ,  $D = 8$ ,  $k_2 = 0.6$ ,  $k_3 = 1.5$ , and  $\beta = \pi/4$ : curve 0,  $n = 0$ , angle  $\varphi_m = 0$ ; curve 1,  $n = 1$ , angle  $\varphi_m = \pi/2$ ; curve 2,  $n = 2$ , angle  $\varphi_m = \pi$ .

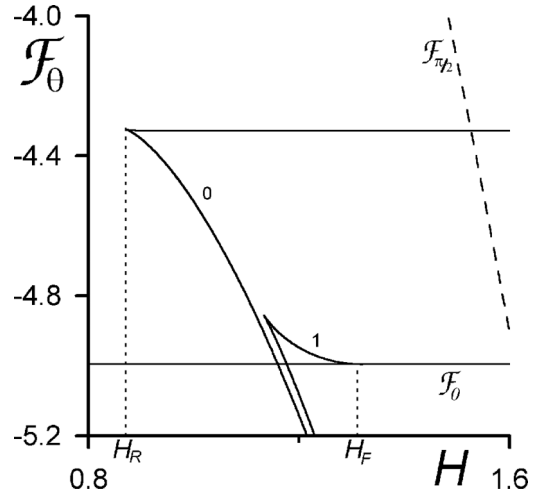


FIG. 9. Dependence of  $\mathcal{F}_\theta$  on magnetic field strength  $H$  for  $w = 5$ ,  $D = 5$ ,  $k_2 = 0.6$ ,  $k_3 = 1.5$ , and  $\beta = \pi/4$ : curve 0,  $n = 0$ , angle  $\varphi_m = 0$ ; curve 1,  $n = 1$ , angle  $\varphi_m = \pi/2$ .

direction of a field  $H$ , and at  $H \geq H_S$  the director is oriented along the field  $H$  in the cell. Thus, the transition from the cholesteric into the homeotropic nematic state, caused by the increase of the magnetic field strength  $H$ , is a second order phase transition.

The reverse, a decrease in the magnetic field strength  $H$ , causes, beginning with  $H \leq H_S$ , a second order transition from the homeotropic nematic phase into the confocal cholesteric state with  $\varphi_m = \pi/2$  ( $n = 1$ ), which exists up to  $H \geq H_R$ , and at  $H = H_R$  the conical spiral structure transforms in the planar cholesteric state, in which  $\varphi_m = \pi$  ( $n = 2$ ).

In Figs. 8 and 9 the thickness of the layer  $D = 5$ ; i.e., at  $0 \leq H \leq H_F$  there is a planar cholesteric state in the layer with  $\varphi_m = \pi/2$  (see thick curve with index 1 in Fig. 4). At  $H \geq H_F$  the planar alignment transforms in a stepwise fashion in the

confocal state with  $\varphi_m = 0$ : the spiral structure of the CLC disappears, and the total turn of the director on the thickness of the layer is determined only by the relative turn of the boundaries of the layer ( $\Delta\varphi = 2\varphi_S$ ). The further increase of the field causes at  $H \rightarrow H_S$  the transition into the homeotropic nematic state.

Decrease of the field  $H$ , beginning with  $H \leq H_S$ , leads to the replacement of the homeotropic nematic alignment by the confocal cholesteric state with  $\varphi_m = 0$ , which at  $H = H_R$  transforms in a stepwise fashion into the planar cholesteric state with  $\varphi_m = \pi/2$ .

The jumps of  $\theta_m$  in Figs. 6 and 8 at the increase or decrease of the field  $H$  occur at the transitions between the planar cholesteric state and the confocal cholesteric state, but the transition between the cholesteric phase and the nematic phase is carried out in a continuous way, i.e., without jump of  $\theta_m$ ; therefore, the cholesteric-homeotropic nematic transition shown in Figs. 6–9 is a transition of second order.

The decrease of the anchoring energy  $w$  influences the character of the phase transition from the planar cholesteric state into the homeotropic nematic state. At a relatively large value of  $w$  this transition is accompanied by the appearance of the intermediate confocal state; in this case for the given thickness  $D$  the following relation for the threshold fields  $H_F < H_S$  (see Figs. 4 and 6–9) takes place. According to the numerical calculations, at the decrease of the anchoring energy we obtain  $H_S < H_F$ , beginning with some value  $w^*$  (see Fig. 5). In this case the solutions describing the confocal state look similar to the curve 2 in Fig. 4 for any values of the thickness  $D$  of the layer. Thus the total energy of such a confocal state exceeds the energies of the planar and homeotropic states; i.e., the confocal state is unstable and for the given thickness  $D$  the increase of  $H$  causes the transition from the planar cholesteric state directly into the homeotropic nematic state at  $H = H_i^*$ , and the decrease of  $H$  from the part of large values results at  $H \leq H_i^*$  in returning to a nematic-planar cholesteric transition. In this case the transition is of first order. The value of the field strength, at which there

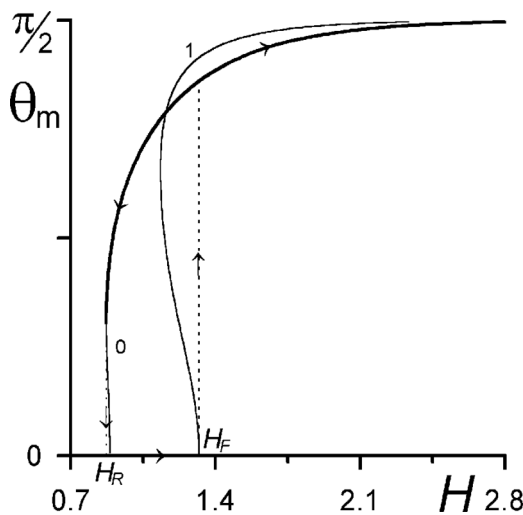


FIG. 8. Dependence of the angle  $\theta_m$  on the magnetic field strength  $H$  for  $w = 5$ ,  $D = 5$ ,  $k_2 = 0.6$ ,  $k_3 = 1.5$ , and  $\beta = \pi/4$ : curve 0,  $n = 0$ , angle  $\varphi_m = 0$ ; curve 1,  $n = 1$ , angle  $\varphi_m = \pi/2$ .

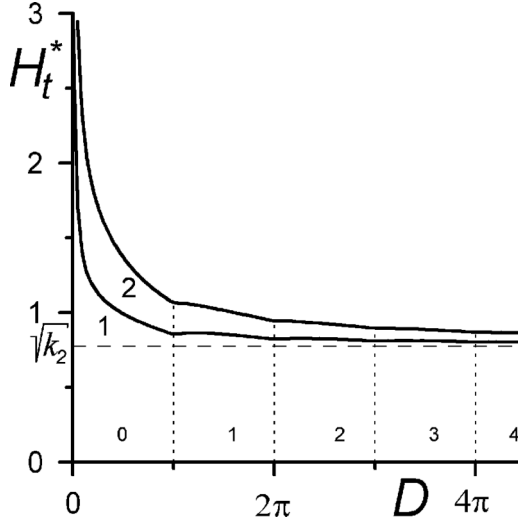


FIG. 10. Dependence of  $H_t^*$  on the layer thickness  $D$  for  $k_2 = 0.6$ ,  $k_3 = 1.5$ , and  $\beta = \pi/4$ : curve 1,  $w = 0.3$ ; curve 2,  $w = 1$ .

is this phase transition, for the given thickness  $D$  is determined from the equality between the total energies (26) and (27):

$$H_t^* = \left[ k_2 + \frac{2w}{D} \cos^2(\beta - \varphi_S) - \frac{w^2}{4k_2} \sin^2 2(\beta - \varphi_S) \right]^{1/2}, \quad (61)$$

where the value of  $\varphi_S$  is determined by Eq. (25) in which the angle  $\varphi_m$  can be found from Eq. (43). The value of anchoring energy  $w^*$ , at which  $H_F \sim H_S$ , one can estimate from the comparison of the asymptotic expressions (54) and (60):

$$w^* \sim \sqrt{k_3^2 - k_2^2}. \quad (62)$$

As the characteristic values of the modules of orientational elasticity belong to the intervals [2]

$$0.5 < \frac{K_{33}}{K_{11}} < 3.0, \quad 0.5 < \frac{K_{22}}{K_{11}} < 0.8, \quad (63)$$

then, using Eq. (8), we obtain

$$0 < w^* \leq 2.958. \quad (64)$$

Hence, at  $K_{11} \sim 1 \times 10^{-7}$  dyn and  $q_0 \sim 1 \times 10^3 - 1 \times 10^4$  cm $^{-1}$  the azimuthal anchoring energy should be relatively small:  $0 < W_a < 1 \times 10^{-3}$  erg/cm $^2$ . We note, that, as it is known [8], the typical values are  $W_a \sim 1 \times 10^{-3} - 1$  erg/cm $^2$ .

Thus, at  $w > w^*$  the planar cholesteric-homeotropic nematic phase transition is accompanied by the appearance of the intermediate state with confocal ordering, i.e., is a second order transition, and at  $w \leq w^*$  the planar state transforms into a homeotropic state without the appearance of a conical spiral structure, i.e., as a first order transition. We note that Eq. (62) is carried out better, the greater the thickness of the layer  $D$ .

In Fig. 10 the dependencies  $H_t^*$  on the thickness  $D$  for different anchoring energies  $w < w^*$  are depicted:  $w = 0.3$  (curve 1) and  $w = 1$  (curve 2). As seen from Eq. (61), at  $D \rightarrow 0$  the magnetic field strength  $H_t^* \rightarrow \infty$ , and at  $D \rightarrow \infty$  the threshold value  $H_t^* \rightarrow \sqrt{k_2}$  (since  $\varphi_S \rightarrow \beta$ ). In the area below the curve the planar cholesteric state exists, and

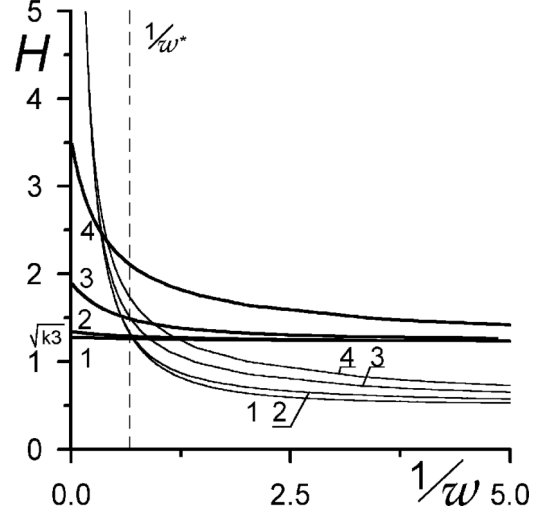


FIG. 11. Dependence of  $H_F$  (thick lines) and  $H_S$  (thin lines) on the inverse anchoring energy  $1/w$  for  $k_2 = 0.6$ ,  $k_3 = 1.5$ , and  $\beta = \pi/4$ : curve 1,  $D = 8$ ; curve 2,  $D = 5$ ; curve 3,  $D = 2$ ; curve 4,  $D = 1$ .

above the curve the homeotropic nematic one exists. Thus, in the planar state for the given thickness  $D$  the angle  $\varphi_m$  is determined by Eqs. (22) and (43); in Fig. 10 the areas of different values of  $\varphi_m$  are separated from each other by vertical dashed lines, where the indices correspond to the integer values of  $n$  [see Eq. (43)].

In Fig. 11 the dependencies of the Fréedericksz field  $H_F$  (thick lines) and saturation field  $H_S$  (thin lines) on the inverse energy of coupling  $1/w$  for different values of the layer thickness  $D$  are shown; the vertical dashed line corresponds to the value  $1/w^*$ . As seen from this figure, relationship (62) is carried out better, the greater the value of  $D$ ; i.e., at  $w > w^*$  the threshold values of the field satisfy the inequality  $H_S > H_F$  (otherwise,  $H_S \leq H_F$ ). At small  $D$  the relationship (62) works badly (see curve 4 in Fig. 11). At  $w \rightarrow \infty$  (rigid anchoring)  $H_S \rightarrow \infty$ ; i.e., in the case of rigid planar anchoring it is impossible to reorient the director of the CLC in a homeotropic state. At  $w \rightarrow 0$  the threshold fields achieve the following values:  $H_F \rightarrow \sqrt{k_3}$  [it follows from Eqs. (50) and (51)] and  $H_S \rightarrow k_2/\sqrt{k_3}$  [see Eq. (60)].

### III. INFLUENCE OF POLAR ANCHORING STRENGTH

Let us consider the general form of the anchoring potential [5], including the polar  $W_p$  and azimuthal  $W_a$  energies of coupling. For this purpose we write Eqs. (4) and (5) as follows:

$$z = 0 : F_S = -\frac{W_p}{2} (\mathbf{n} \cdot \mathbf{e}_z)^2 - \frac{W_a}{2} (\mathbf{n} \cdot \mathbf{e}_{s1})^2, \quad (65)$$

$$z = d : F_S = -\frac{W_p}{2} (\mathbf{n} \cdot \mathbf{e}_z)^2 - \frac{W_a}{2} (\mathbf{n} \cdot \mathbf{e}_{s2})^2. \quad (66)$$

Here the designations are the same as in Sec. II A;  $W_p$  and  $W_a$  are the so-called polar and azimuthal anchoring strengths, respectively. As seen from Eqs. (65) and (66), at  $W_a > W_p$  these potentials have a minimum at  $\mathbf{n} \parallel \mathbf{e}_{s1(2)}$ , i.e., they describe the anchoring interaction with the axis of easy

orientation lying at the boundary of a layer (planar conditions of coupling), and at  $W_a < W_p$  the easy axis is directed along a normal to the boundaries (homeotropic conditions of coupling,  $\mathbf{n} \parallel \mathbf{e}_z$ ). For clarity we suppose that  $W_a > W_p$ ; i.e., in the absence of a magnetic field there is planar alignment in a cell. Minimization of the total energy functional (2) in which the volume contribution is defined by Eq. (3), and the surface one is defined by Eqs. (65) and (66), results in new relationships determining the threshold values of a magnetic field and a thickness of a layer at which there are orientational transitions between three possible kinds of one-dimensional distributions of the director field (1).

The expressions of Sec. II C, determining the critical parameters of the system at which there is a transition between the planar cholesteric state [ $\theta(z) = 0$ ] and the confocal state [ $0 < \theta(z) < \pi/2$ ], with the aid of Eq. (65) can be written now as

$$D = \frac{4k_2(\varphi_m + \varphi_S)}{2k_2 + w_a \sin 2(\beta - \varphi_S)}, \quad (67)$$

$$\begin{aligned} & \frac{\sqrt{\gamma(\varphi_S)}}{2k_2[w_a \cos^2(\beta - \varphi_S) - w_p]} \\ &= \cot \left\{ \frac{(\varphi_m + \varphi_S)\sqrt{\gamma(\varphi_S)}}{2k_2 + w_a \sin 2(\beta - \varphi_S)} \right\}. \end{aligned} \quad (68)$$

Here the designations are the same, as in Sec. II A, and  $w_a = W_a/(q_0 K_{11})$  and  $w_p = W_p/(q_0 K_{11})$ . Equations (67) and (68) and the function

$$\begin{aligned} \gamma(\varphi_S) = & [w_a \sin 2(\beta - \varphi_S) + 2k_2] \\ & \times [w_a(2k_2 - k_3) \sin 2(\beta - \varphi_S) - 2k_2 k_3] + 4k_2^2 H_F^2 \end{aligned}$$

at  $w_a = w$  coincide with Eqs. (50) and (52) obtained in Sec. II A, and at  $w_p = 0$  Eqs. (67) and (68) are reduced to Eqs. (50) and (51). Just as in Sec. II A [see Eq. (25)], Eq. (67) at the given layer thickness  $D$  determines the values of the angle  $\varphi_S$  in the planar state. The values of  $\varphi_m$  in Eqs. (67) and (68) should satisfy relation (22) in which the integer  $n$  is determined by Eq. (43). If we choose  $w_a = 0$  (the case of azimuthal degeneration of the easy axis), Eqs. (67) and (68) can be written as follows:

$$D = \frac{1}{\sqrt{k_3 - H_F^2}} \ln \left\{ \frac{\sqrt{k_3 - H_F^2} + w_p}{\sqrt{k_3 - H_F^2} - w_p} \right\}. \quad (69)$$

With the increase of the layer thickness ( $D \rightarrow \infty$ ) the Fréedericksz field  $H_F$ , determined by Eqs. (67) and (68), or Eq. (69), just as in Sec. II C, has the asymptotic value  $H_F \rightarrow \sqrt{k_3}$  [see Eq. (54)].

In Fig. 12 the dependence of the Fréedericksz field  $H_F$  on the thickness  $D$  is shown. The family of dashed and thick lines (the designations are the same as in Fig. 4; see Sec. II C) corresponds to the cases  $w_a = 5$  and  $w_p = 0$  in Fig. 12. The family of continuous and thick lines in Fig. 12 corresponds to the case  $w_a = 5$  and  $w_p = 4.5$ . Each dashed or continuous line of the family with the integer index in Fig. 12 represents the solution of Eqs. (67) and (68), where the angle  $\varphi_m$  is determined by Eq. (22) with  $n$  equal to the index of the curve.

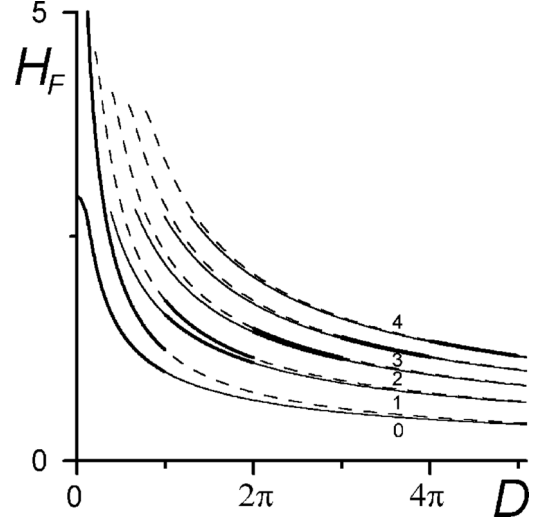


FIG. 12. Dependence of the field  $H_F$  on the thickness  $D$  for  $k_2 = 0.6$ ,  $k_3 = 1.5$ ,  $\beta = \pi/4$ , and  $w_a = 5$ : dashed lines,  $w_p = 0$ ; solid lines,  $w_p = 4.5$ .

Because with the increase of the layer thickness  $D$  the number of half turns of the spiral should be increased (which causes the increase of  $\varphi_m$  and increase of  $n$ ; see Sec. II C), the actual dependence  $H_F(D)$  in Fig. 12 corresponds to thick parts of the curves for which relationship (43) is carried out. As seen from Fig. 12, the increase of polar coupling energy  $w_p$  leads to a slight influence on the dependence  $H_F(D)$ : the difference between the values  $H_F$  for  $w_p = 0$  and  $w_p \neq 0$  decreases with the increase of the thickness  $D$  (see thick plots of curves in Fig. 12).

Equations (59), determining the threshold characteristics of the transition in a homeotropic nematic state, for the case of anchoring interaction (65) is as follows:

$$\begin{aligned} D &= \frac{4k_3}{a_1} \ln \left\{ \frac{a_1 \alpha_{S1} + \sqrt{a_1^2 (\alpha_{S1}^2 + 1) + b_1^2}}{\sqrt{a_1^2 + b_1^2}} \right\}, \\ \varphi_m + \varphi_{S0} &= \arctan \left\{ \frac{\alpha_{S1} b_1}{\sqrt{a_1^2 (\alpha_{S1}^2 + 1) + b_1^2}} \right\} + \frac{k_2 D}{k_3} \\ &= 2(\alpha_{S1}^2 + 1) [w_a \cos^2(\beta - \varphi_{S0}) - w_p], \end{aligned} \quad (70)$$

where  $a_1 = \sqrt{4(H_S^2 k_3 - k_2^2)}$  and  $b_1 = w_a(\alpha_{S1}^2 + 1) \sin 2(\beta - \varphi_{S0})$ . As already marked in Sec. II E, the transition in a homeotropic state is accompanied by total unwinding of the CLC spiral (the number of half turns of the spiral  $n = 0$ ); therefore, in Eqs. (70) the angle  $\varphi_m = 0$ . Equations (70) at  $w_p = 0$  coincide with Eqs. (59), and in the case of azimuthal degeneration of the easy axis ( $w_a = 0$ ) Eqs. (70) can be written in the following form:

$$D = \frac{2k_3}{\sqrt{k_2^2 - H_S^2 k_3}} \arctan \left\{ \frac{w_p}{\sqrt{k_2^2 - H_S^2 k_3}} \right\}. \quad (71)$$

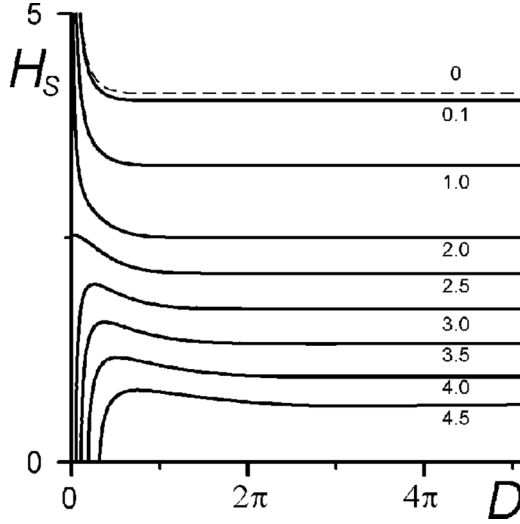


FIG. 13. Dependence of the field  $H_S$  on the thickness  $D$  for  $k_2 = 0.6$ ,  $k_3 = 1.5$ ,  $\beta = \pi/4$ , and  $w_a = 5$ ; the numbers in the curves correspond to  $w_p$ .

At  $D \rightarrow \infty$  the field strength  $H_S \rightarrow H_S^*$ , where the value  $H_S^*$ , instead of that in Eq. (60), is determined now as

$$H_S^* = \sqrt{\frac{k_2^2 + (w_a - w_p)^2}{k_3}}, \quad (72)$$

which follows from Eqs. (70); thus,  $\varphi_{S0} \rightarrow \beta$  and  $\alpha_{S1} \rightarrow \infty$  (see Sec. IID).

At the limit  $\varphi_{S0} \rightarrow 0$  and  $\alpha_{S1} \rightarrow 0$  Eqs. (70) have the solution  $D \rightarrow 0$ , for which

$$w_a \cos^2 \beta = w_p,$$

$$H_S = \frac{1}{k_3} \sqrt{k_2^2 k_3 + w_a \sin 2\beta \left( k_2^2 + \frac{1}{4} k_3 \sin 2\beta \right)}. \quad (73)$$

These formulas describe the asymptotic behavior of curve 2.5 in Fig. 13 at  $D \rightarrow 0$ . In the case of  $w_a \cos^2 \beta > w_p$  at  $D \rightarrow 0$  from Eqs. (70) we obtain that  $H_S \rightarrow \infty$  (curves 0, 0.1, 1.0, and 2.0 in Fig. 13). At  $w_a \cos^2 \beta < w_p$  the saturation state is achieved in thin layers owing to the influence of the boundaries (curves 3.0, 3.5, 4.0, and 4.5 in Fig. 13): the magnetic field  $H_S$  vanishes at the thickness

$$D = \frac{2k_3}{k_2} \arctan \left\{ \frac{2\alpha_{S1} k_2}{\sqrt{b_1^2 - 4k_2^2 (\alpha_{S1}^2 + 1)}} \right\}. \quad (74)$$

In Fig. 13 the evolution of the dependence of the saturation field  $H_S$  on the thickness  $D$  at the increase of the polar energy of coupling  $w_p$  is shown. The dashed curve in Fig. 13 corresponds to  $w_a = 5$  and  $w_p = 0$  (see Sec. IIC, Fig. 4). As seen from Figs. 12 and 13 and Eq. (60), the increase of the polar energy of coupling  $w_p$  causes a significant decrease of the saturation field  $H_S$ , but almost does not change the value of the Fréedericksz field  $H_F$ . It allows us to choose such values of  $w_a$  and  $w_p$  at which  $H_F < H_S$ , or  $H_F > H_S$ . In the latter case,

as marked above, the cholesteric-nematic transition becomes a first order transition.

For large thicknesses ( $D \rightarrow \infty$ ), as already marked, the field  $H_F \rightarrow \sqrt{k_3}$ , and  $H_S$  is determined by Eq. (72); therefore, the relationship at which  $H_F \approx H_S$  can be written as follows:

$$(k_3^2 - k_2^2) \approx (w_a - w_p)^2. \quad (75)$$

Hence, at  $(k_3^2 - k_2^2) < (w_a - w_p)^2$  the cholesteric-nematic transition is a second order transition ( $H_F < H_S$ ), and at  $(k_3^2 - k_2^2) > (w_a - w_p)^2$  it is a first order transition ( $H_F > H_S$ ).

#### IV. INFLUENCE OF DEGENERATION OF THE EASY ORIENTATION AXIS ON THE CHOLESTERIC-NEMATIC TRANSITION

Let us consider the features of phase transition between the cholesteric and homeotropic nematic states in a layer with twofold degeneration of an easy orientation axis on the boundaries. The homogeneous magnetic field  $\mathcal{H} = (0, 0, \mathcal{H})$  is directed along the  $z$  axis, and the anisotropy of diamagnetic susceptibility is  $\chi_a > 0$ . For the description of anchoring interaction, instead of Eq. (4) we use the following potential [47]:

$$z = 0: \quad F_S = \frac{W}{2} [1 - (\mathbf{n} \cdot \mathbf{e}_{s1})^2] [1 - (\mathbf{n} \cdot \mathbf{e}_z)^2], \quad (76)$$

$$z = d: \quad F_S = \frac{W}{2} [1 - (\mathbf{n} \cdot \mathbf{e}_{s2})^2] [1 - (\mathbf{n} \cdot \mathbf{e}_z)^2], \quad (77)$$

which has a minimum at  $\mathbf{n} \parallel \mathbf{e}_{s1(2)}$ , or at  $\mathbf{n} \parallel \mathbf{e}_z$ , i.e., it describes the twofold degeneration of the easy axis of orientation;  $W > 0$  is the surface density of the coupling energy of CLC molecules with the boundaries of a cell. The director field  $\mathbf{n}(\mathbf{r})$  is searched as in Eq. (1). The designations used in the present section coincide with the designations made in Sec. IIA [see Eqs. (4)–(15)].

Operating just as in Sec. IIA, one can obtain the equilibrium distribution of the director field. For the dependencies  $\theta(z)$  and  $\varphi(z)$ , and the angles  $\theta_m$  and  $\varphi_S$ , the obtained equations coincide with Eqs. (32), (33), and (35) from Sec. IIA, in which the function  $A(\theta)$  is determined by expression (34), and the integration constant

$$C_2 = \frac{w}{2} \cos^4 \theta_S \sin 2(\beta - \varphi_S). \quad (78)$$

The equation for the determination of the angle  $\theta_S$  looks like

$$-\frac{f(\theta_S)}{\sqrt{A(\theta_S)}} = \frac{w}{2} \sin 2\theta_S [1 - 2 \cos^2 \theta_S \cos^2(\beta - \varphi_S)]. \quad (79)$$

The angle  $\varphi_m$  accepts the discrete series of values determined by Eq. (22).

The equations of equilibrium have three types of solutions corresponding to different kinds of structures: the planar CLC, the confocal CLC, and the homeotropic nematic structure.

In the planar state [ $\theta(z) = 0$ ] the values of the angles  $\varphi_S$  and  $\varphi_m$  are determined by the equations which coincide with Eqs. (25), (22), and (43). The expression for the total energy in the planar state  $\mathcal{F}_0 \equiv \mathcal{F}/(K_{11}q_0S)$  looks like

$$\mathcal{F}_0 = \frac{D}{8k_2} w^2 \sin^2 2(\beta - \varphi_S) + w \sin^2(\beta - \varphi_S). \quad (80)$$

The total energy (80) does not depend explicitly on the magnetic field  $H$  and achieves the lowest value  $\mathcal{F}_0 = 0$  only in the case when the thickness of a layer satisfies relation (40). For the infinite cholesteric layer ( $D \rightarrow \infty$ ) the total energy  $\mathcal{F}_0 \rightarrow 0$ , since in this case the pitch of the spiral  $p \rightarrow p_0$ .

The total energy of the homeotropic state  $\mathcal{F}_{\pi/2} [\theta(z) = \pi/2]$  is determined by the equation which coincides with Eq. (27). For the case of the confocal ordering [ $0 < \theta(z) < \pi/2$ ] the total energy  $\mathcal{F}_\theta$  is expressed by Eq. (38), in which the last item (the contribution of the anchoring interaction) can be written as  $w \cos^2 \theta_S [1 - \cos^2 \theta_S \cos^2(\beta - \varphi_S)]$ .

For the determination of the threshold values for the thickness  $D$  and the magnetic field strength  $H$  (see Secs. II C and II D) one can consider the above-described equations of the CLC equilibrium state at  $\theta_m \rightarrow 0$  (the Fréedericksz field) and at  $\theta_m \rightarrow \pi/2$  (the saturation field).

In the limit  $\theta_m \rightarrow 0$  the equations of equilibrium become

$$D = \frac{4k_2(\varphi_m + \varphi_S)}{w \sin 2(\beta - \varphi_S) + 2k_2}, \quad (81)$$

$$\frac{\sqrt{\gamma(\varphi_S)}}{2wk_2 \cos 2(\beta - \varphi_S)} = \cot \left\{ \frac{\sqrt{\gamma(\varphi_S)}(\varphi_m + \varphi_S)}{w \sin 2(\beta - \varphi_S) + 2k_2} \right\}. \quad (82)$$

Here the function  $\gamma(\varphi_S)$  is defined by Eq. (52), and the values of  $\varphi_m$  are determined by Eqs. (22) and (43). Equations (81) and (82) determine the threshold values of the CLC material parameters, the thickness  $D$ , and the magnetic field strength  $H$  beginning with which there is confocal ordering in a layer. For example, at the increase of the thickness  $D$  up to the value determined by Eqs. (81) and (82), the planar structure exists, and above this value, the confocal solution appears. If the thickness  $D$  is fixed, Eqs. (81) and (82) determine the value of the so-called Fréedericksz field  $H_F$  (see Sec. II C) such that at  $H < H_F$  there is a planar CLC structure, and at  $H \geq H_F$  there is a confocal CLC state.

In order to determine the threshold values of the thickness  $D$  and magnetic field  $H$  at which a homeotropic state could exist in a layer, we consider the equations of state in the limit  $\theta_m \rightarrow \pi/2$ . As a result, we obtain the equation

$$D = \frac{2k_3}{\sqrt{k_2^2 - H_S^2 k_3}} \arctan \left( \frac{w}{\sqrt{k_2^2 - H_S^2 k_3}} \right). \quad (83)$$

For the given thickness  $D$ , expression (83) determines the so-called saturation field  $H_S$ , such that at  $H > H_S$  there is a homeotropic nematic state in a layer, and at  $H \leq H_S$  there is a confocal cholesteric state.

In Fig. 14 the Fréedericksz field  $H_F$  (continuous lines) and the saturation field  $H_S$  (dashed curve) are shown as functions of the layer thickness  $D$  (see also Figs. 4 and 5). The integer indices in Fig. 14 correspond to the values of  $n$  in Eq. (43). The area of existence of the confocal solution is limited by the curves  $H_F(D)$  and  $H_S(D)$ , and, as seen from Fig. 14, for any thickness  $D$  the inequality  $H_S < H_F$  always takes place (the similar case is considered in Secs. II C and II E). Numerical calculations based on the comparison of the total energies of the planar state  $\mathcal{F}_0$  [Eqs. (80)], the confocal state  $\mathcal{F}_\theta$  and the homeotropic state  $\mathcal{F}_{\pi/2}$  in the area of a confocal solution existence, show that the solution describing the conical spiral

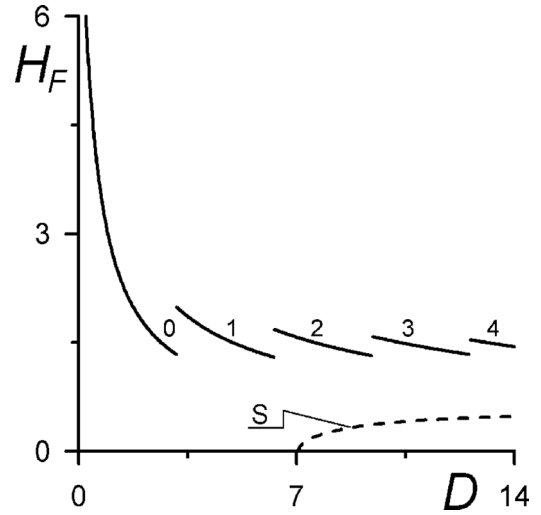


FIG. 14. Dependence of the Fréedericksz field  $H_F$  and saturation field  $H_S$  (dashed line) on the thickness  $D$  of the layer for  $w = 5$ ,  $k_2 = 0.8$ ,  $k_3 = 2.0$ , and  $\beta = \pi/4$ . The integer indices are the values of  $n$ .

ordering in a layer is absolutely unstable for any chosen values of the CLC material parameters. Thus, the total energy of the confocal state  $\mathcal{F}_\theta$  appears to be always higher than the energies of the planar and homeotropic states. Hence, the orientational phase transition from the planar cholesteric state into the homeotropic nematic state takes place without the appearance of an intermediate confocal ordering; i.e., this phase transition is of first order. At the transition point the energies of the planar and homeotropic states are equal to each other; i.e., two states with  $\theta(z) = 0$  and  $\theta(z) = \pi/2$  are not divided by the potential barrier. The values of the critical parameters at which the phase transition takes place are determined from the equality  $\mathcal{F}_0 = \mathcal{F}_{\pi/2}$ . In particular, if the variable parameter is the magnetic field  $H$ , then the expression

$$H_t^* = \left[ k_2 - \frac{2w}{D} \sin^2(\beta - \varphi_S) - \frac{w^2}{4k_2} \sin^2 2(\beta - \varphi_S) \right]^{1/2} \quad (84)$$

determines the critical magnetic field strength  $H_t^*$ , such that at  $H < H_t^*$  there is a planar state in a layer, and at  $H \geq H_t^*$  the phase transition of first order into a homeotropic nematic state occurs. The value of  $\varphi_S$  in Eq. (84) is determined by expression (25) in which the angle  $\varphi_m$  can be found from Eq. (43).

Thus, the presence of twofold degeneration of the easy axis of orientation on the boundaries of a layer [see Eqs. (76) and (77)] excludes the appearance of confocal cholesteric ordering in a layer at any possible values of material parameters. The orientational phase transition in this case is the transition of first order at which the planar cholesteric state discontinuously changes with homeotropic nematic state. If this phase transition is caused by the variation of a magnetic field, Eq. (84) determines the critical field of such a transition. Recall that in the case of a planar anchoring of the director at the boundaries of the layer [see Eqs. (4) and (5)] the first order transition is possible only in that case, when the energy of coupling  $w < w^*$ , where  $w^*$  is determined by Eq. (62), i.e., at relatively small values of the azimuthal coupling energy.

## V. CONCLUSIONS

In the present work within the framework of continuum theory magnetic-field-induced cholesteric-nematic transition in a layer with soft planar coupling between the director and the boundaries of a layer has been investigated. It has been supposed that the helical axis of a CLC and a magnetic field are directed along a normal to the layer, and diamagnetic anisotropy is positive. It is shown that, depending on the thickness of a layer or magnetic field strength, the homogeneous homeotropic nematic state or cholesteric state of a planar or confocal type can exist in the layer. In the latter case the director of the CLC is oriented under some angle to the spiral axis and forms the conical helicoidal structure.

It has been established that the increase in the thickness of a layer in the planar cholesteric state leads to a stepwise increase in the number of half turns of the spiral in the cell that causes the jumps of average over a cell transverse components of a magnetic susceptibility tensor  $\langle\chi_{ij}\rangle$  of the CLC. Experimental measuring of such jumps allows one, using Eqs. (48) and (49), to estimate the azimuthal energy of coupling  $W_a$ .

It is shown that at a given thickness of a layer the increase in magnetic field causes the orientational phase transition from the planar cholesteric state to a homeotropic nematic state; thus, depending on the value of the coupling energy the intermediate confocal cholesteric structure can either be observed or not observed, i.e., the phase transition can be a transition of both second and first order. For the case of large thickness the threshold value of azimuthal energy of coupling  $W_a^* = q_0\sqrt{K_{33}^2 - K_{22}^2}$  is determined, such that at  $W_a > W_a^*$  the planar cholesteric-homeotropic nematic phase transition is accompanied by the appearance of the intermediate state with confocal ordering, i.e., is a transition of second order, and at  $W_a \leq W_a^*$  the planar state changes by homeotropic nematic state without appearance of a conical spiral structure, i.e., as a first order transition. It is shown that in the case of second order transition the transition in the homeotropic state is accompanied by unwinding of the CLC spiral structure; i.e., the increase in the magnetic field directed along the axis of a CLC spiral causes a decrease of the number of half turns of the director around the axis of a spiral in the layer is not the external parameter but is determined by the relation between the thickness of the layer and the value of the intrinsic CLC pitch.

The threshold characteristics are determined, at which there are the transitions from the planar cholesteric state into the

confocal state (the Fréedericksz field) and from the confocal state into the homeotropic nematic state (the saturation field) for anchoring potential (65). It is shown that in the case of planar coupling ( $W_a > W_p$ ) the increase in the polar energy of coupling  $W_p$  insignificantly changes the dependence of the Fréedericksz field  $\mathcal{H}_F$  on the layer thickness, but considerably reduces the saturation field  $\mathcal{H}_S$  at which there is a transition into the homeotropic nematic state (see Fig. 13). It allows one to choose such values of  $W_a$  and  $W_p$  at which the phase transition becomes the transition either of first or second order. In particular, for the case of large thickness of the layer at  $q_0^2(K_{33}^2 - K_{22}^2) > (W_a - W_p)^2$  the cholesteric-nematic transition will be a first order transition.

In the present paper we have considered the anchoring potential, Eqs. (76) and (77), which corresponds to twofold degeneration of the axis of easy orientation. The presence of two axes of easy orientation, one lying in the plane of the layer and the second oriented along the normal to the layer, leads to the fact that the cholesteric-nematic phase transition is always a transition of first order, i.e., the planar cholesteric structure transforms in a stepwise fashion into the homeotropic nematic state, and the confocal state is absolutely unstable. From the comparison of the total energies of the planar and homeotropic states the critical value of a magnetic field  $\mathcal{H}_t^*$  is determined, at which the phase transition takes place: at  $\mathcal{H} < \mathcal{H}_t^*$  there is a planar state in a layer, and at  $\mathcal{H} \geq \mathcal{H}_t^*$  the first order transition in a homeotropic nematic state takes place.

We have studied the cholesteric-nematic phase transition and the stepwise behavior of a cholesteric pitch using the Rapini potential [3] of soft anchoring. As it is known, the Rapini potential is rather good in the case of small deviations of the nematic director from the easy direction. For a large director deviation from the easy direction the so-called Belyakov potential [48–50] is more suitable. Note that a stepwise change of the helical structure corresponds to substantial deviations of the director and, therefore, the Belyakov potential more adequately can describe this phenomenon. In recent work [48] an experimental investigation of the cholesteric structure in a wedge-shaped cell with soft surface anchoring was performed. Such a cell allows one to restore the shape of the surface anchoring potential. From Ref. [48] it follows that apparently a more accurate description of the stepwise behavior can be obtained using the Belyakov potential.

## ACKNOWLEDGMENT

This work was partially supported by Grant No. 16-42-590539 from the Russian Foundation for Basic Research.

- 
- [1] P. G. de Gennes, *The Physics of Liquid Crystals* (Clarendon, Oxford, 1974).
  - [2] L. M. Blinov, *Structure and Properties of Liquid Crystals* (Springer, Dordrecht, 2011).
  - [3] A. Rapini and M. Papoular, *J. Phys. (Paris)*, **Colloq.** **30**, C4-54 (1969).
  - [4] R. Barberi, J. J. Bonvent, M. Giocondo, M. Iovane, and A. L. Alexe-Ionescu, *J. Appl. Phys.* **84**, 1321 (1998).
  - [5] S. V. Shiyonovskii, A. Glushchenko, Yu. Reznikov, O. D. Lavrentovich, and J. L. West, *Phys. Rev. E* **62**, R1477 (2000).
  - [6] K. H. Yang and C. Rosenblatt, *Appl. Phys. Lett.* **43**, 62 (1983).
  - [7] M. I. Barnik, L. M. Blinov, T. V. Korkishko, V. A. Umanskii, and V. G. Chigrinov, *Zh. Eksp. Teor. Fiz.* **85**, 176 (1983) [*Sov. Phys. JETP* **58**, 102 (1983)].
  - [8] L. M. Blinov, A. Yu. Kabaenkov, V. V. Lebedev, and A. A. Sonin, *Izvestia AN USSR, Ser. Phys.* **53**, 1948 (1989).

- [9] P. Jagemalm, G. Barbero, L. Komitov, and A. K. Zvezdin, *Phys. Rev. E* **58**, 5982 (1998).
- [10] H. A. van Sprang and J. L. M. van de Venne, *J. Appl. Phys.* **57**, 175 (1985).
- [11] H. A. van Sprang and P. A. Breddels, *J. Appl. Phys.* **60**, 968 (1986).
- [12] Seong-Woo Suh, Sung Tae Shin, and Sin-Doo Lee, *Mol. Cryst. Liq. Cryst.* **302**, 163 (1997).
- [13] A. Sugimura, G. R. Luckhurst, and Ou-Yang Zhong-can, *Phys. Rev. E* **52**, 681 (1995).
- [14] J. Brox, G. Vertogen, and E. W. C. van Groesen, *Z. Naturforsch.* **38**, 1 (1983).
- [15] J. P. Hurault, *J. Chem. Phys.* **59**, 2068 (1973).
- [16] H. Hervet, J. P. Hurault, and F. Rondelez, *Phys. Rev. A* **8**, 3055 (1973).
- [17] V. G. Chigrinov, V. V. Belyaev, S. V. Belyaev, and M. F. Grebenkin, *Zh. Eksp. Teor. Fiz.* **77**, 2081 (1979) [*Sov. Phys. JETP* **50**, 994 (1979)].
- [18] G. Vertogen and E. W. C. van Groesen, *J. Chem. Phys.* **76**, 2043 (1982).
- [19] G. Cohen and R. M. Hornreich, *Phys. Rev. A* **41**, 4402 (1990).
- [20] M. E. Becker, J. Nehring, and T. J. Scheffer, *J. Appl. Phys.* **57**, 4539 (1985).
- [21] W. Zhao, C.-X. Wu, and M. Iwamoto, *Phys. Rev. E* **62**, R1481 (2000).
- [22] W. Zhao, C.-X. Wu, and M. Iwamoto, *Phys. Rev. E* **65**, 031709 (2002).
- [23] A. Yu. Val'kov, E. V. Aksenova, and V. P. Romanov, *Phys. Rev. E* **87**, 022508 (2013).
- [24] H. Zink and V. A. Belyakov, *JETP* **85**, 285 (1997).
- [25] V. A. Belyakov and E. I. Kats, *JETP* **91**, 488 (2000).
- [26] V. A. Belyakov, *JETP Lett.* **76**, 88 (2002).
- [27] V. A. Belyakov, P. Oswald, and E. I. Kats, *JETP* **96**, 915 (2003).
- [28] V. A. Belyakov, I. W. Stewart, and M. A. Osipov, *JETP* **99**, 73 (2004).
- [29] V. A. Belyakov, I. W. Stewart, and M. A. Osipov, *Phys. Rev. E* **71**, 051708 (2005).
- [30] S. P. Palto, *JETP* **94**, 260 (2002).
- [31] A. M. Scarfone, I. Lelidis, and G. Barbero, *Phys. Rev. E* **84**, 021708 (2011).
- [32] I. Lelidis, G. Barbero, and A. L. Alexe-Ionescu, *Phys. Rev. E* **87**, 022503 (2013).
- [33] G. Barbero and A. M. Scarfone, *Phys. Rev. E* **88**, 032505 (2013).
- [34] G. McKay, *J. Eng. Math.* **87**, 19 (2014).
- [35] V. B. Vinogradov, L. A. Kutulya, Yu. A. Reznikov, V. Yu. Reshetnyak, and A. I. Khizhnyak, *Pisma Zh. Tekh. Fiz.* **15**, 60 (1989).
- [36] V. Vinogradov, A. Khizhnyak, L. Kutulya, Yu. Reznikov, and V. Reshetnyak, *Mol. Cryst. Liq. Cryst.* **192**, 273 (1990).
- [37] I. P. Pinkevich, V. Yu. Reshetnyak, Yu. A. Reznikov, and A. J. Il'in, *Proc. SPIE* **1845**, 510 (1992).
- [38] I. P. Pinkevich, V. Y. Reshetnyak, and M. F. Ledney, *Ukr. Phys. J.* **37**, 218 (1992).
- [39] I. P. Pinkevich, V. Y. Reshetnyak, Y. A. Reznikov, and L. G. Grechko, *Mol. Cryst. Liq. Cryst. Sci. Technol. Sect. A* **222**, 269 (1992).
- [40] P. J. Kedney and J. W. Stewart, *Continuum Mech. Thermodyn.* **6**, 141 (1994).
- [41] I. Lelidis, G. Barbero, and A. M. Scarfone, *Cent. Eur. J. Phys.* **10**, 587 (2012).
- [42] A. D. Kiselev and T. J. Sluckin, *Phys. Rev. E* **71**, 031704 (2005).
- [43] G. McKay, *Eur. Phys. J. E* **35**, 74 (2012).
- [44] P. Schiller, *Liq. Cryst.* **4**, 69 (1989).
- [45] P. Schiller, *Phase Trans.* **29**, 59 (1990).
- [46] R. Hirning, W. Funk, H.-R. Trebin, M. Schmidt, and H. J. Schmiedel, *J. Appl. Phys.* **70**, 4211 (1991).
- [47] A. J. Davidson and N. J. Mottram, *Phys. Rev. E* **65**, 051710 (2002).
- [48] K. Nowicka, D. Dardas, W. Kuczyński, V. A. Belyakov, and D. V. Shmeliyova, *Liq. Cryst.* **41**, 1448 (2014).
- [49] V. A. Belyakov, *Mol. Cryst. Liq. Cryst.* **467**, 155 (2007).
- [50] V. A. Belyakov, *Mol. Cryst. Liq. Cryst.* **489**, 54/[380] (2008).